 

# EXPERIMENTAL SEARCH FOR THE RADIATIVE CAPTURE REACTION $d + d \rightarrow {}^4\mathrm{He}+\gamma$ FROM THE $dd\mu$ MUONIC MOLECULE STATE $J = 1$

*V. V. Baluev*[a], *L. N. Bogdanova*[b], *V. R. Bom*[c], *D. L. Demin*[d*], *C. W. E. van Eijk*[c], *V. V. Filchenkov*[d], *N. N. Grafov*[d], *S. K. Grishechkin*[a], *K. I. Gritsaj*[d], *A. D. Konin*[d], *K. L. Mikhailyukov*[a], *A. I. Rudenko*[d], *Yu. I. Vinogradov*[a], *V. P. Volnykh*[d], *A. A. Yukhimchuk*[a], *S. A. Yukhimchuk*[d]

[a]*Russian Federal Nuclear Center, All-Russian Research Institute of Experimental Physics 607188, Nizhnii Novgorod region, Sarov, Russia*

[b]*State Scientific Center of the Russian Federation "Institute of Theoretical and Experimental Physics" 117218, Moscow, Russia*

[c]*Delft University of Technology Delft 2600 AA, The Netherlands*

[d]*Joint Institute for Nuclear Research 141980, Dubna, Moscow Region, Russia*

Received June 25, 2010

A search for the muon-catalyzed fusion reaction $d + d \rightarrow^4\mathrm{He} + \gamma$ in the $dd\mu$ muonic molecule was performed using the experimental installation TRITON with BGO detectors for $\gamma$-quanta. A high-pressure target filled with deuterium was exposed to the negative muon beam of the JINR Phasotron to detect $\gamma$-quanta with the energy 23.8 MeV. An experimental estimation for the yield of radiative deuteron capture from the $dd\mu$ state $J = 1$ was obtained at the level of $\eta_\gamma \leq 8 \cdot 10^{-7}$ per fusion.

## 1. INTRODUCTION

This experimental work is aimed at the observation of the rare radiative capture reaction

$$d + d \rightarrow {}^4\mathrm{He} + \gamma + 23.8\,\mathrm{MeV} \tag{1}$$

proceeding from the $dd\mu$ muonic molecule state with the total orbital angular momentum $J = 1$. This reaction is one of the deuterium burning processes for which the cross section behavior at low energies (and therefore the astrophysical S-factor) is not well known. A specific feature of the reaction ${}^2\mathrm{H}(d,\gamma){}^4\mathrm{He}$ is its small cross section compared to similar reactions between hydrogen isotopes.

Due to the presence of identical bosons in the entrance channel, reaction (1) selects states with even $L+S$ ($L$ and $S$ are the orbital angular momentum and the total spin of the $dd$ system). This reduces the number of partial waves involved. The allowed transitions are therefore $E1({}^3P_1)$, $M1({}^5D_1)$, $E2({}^1D_2)$, $E2({}^5S_2)$, $E2({}^5D_2)$, and $M2({}^3P_2)$ (we use the standard spectroscopic symbol $({}^{2S+1}L_I)$, where $I$ is the total angular momentum of two deuterons). It was established in beam–target experiments that at energies $E > 400$ keV, reaction (1) proceeds mainly by the quadrupole $E2$ transition from the $d$-wave of the deuteron relative motion to the main component ${}^1S_0$ of the ${}^4\mathrm{He}$ ground state [1].

At very low energies ($E < 100$ keV), due to barrier penetration considerations, the dominant strength should be an $s$-wave $dd$ capture to the small $D$-state admixture of ${}^4\mathrm{He}$ ($E2$ transition). Experiments at beam energies around 100 keV [2] support this expectation.

The next transition strength is expected to be due to $p$-wave capture. For a $p$-wave, only $E1$ and $M2$ tran-

*E-mail: demin@jinr.ru

sitions are allowed. In reaction (1), where the isospin in the initial and final states is zero, the $E1$ transition to the ground state of $^4$He ($S = 0$ or $S = 2$) is suppressed because the leading dipole term of the $E1$ operator is an isovector and vanishes. Besides, the $E1$ transition requires $\Delta S = 1$, and is therefore additionally suppressed. We should expect the $E1$ contribution to be small (of the order of $M2$), in contrast to "usual" capture reactions, such as *pd* or *pt*, where the $E1$ dipole contribution is large.

The $p$-wave effects in the $^2$H($\mathbf{d}, \gamma$)$^4$He reaction were probed by measuring the cross section and angular distributions $\sigma(\theta)$ of the vector $A_y$ and tensor $A_{yy}$ analyzing powers, performed with a polarized deuteron beam with the energy $E_d(lab) = 80$ keV, stopping in a deuterium target [3, 4]. It turned out that over 50 % of the cross section strength at these low energies was due to the $E1$ and $M2$ $p$-wave capture. This finding might affect the low-energy behavior of the total cross section and its extrapolation to sub-Coulomb energies. It would be extremely interesting to observe a manifestation of this $p$-wave in independent measurements.

Muon-catalyzed fusion ($\mu$CF) appears to be helpful in the study of fusion reactions between hydrogen isotopes at lowest energies unattainable in beam–target experiments. In particular, for the *dd* system, it allows selecting the $p$-wave reactions at a virtually zero energy [6]. It is long known that at the deuterium temperature $T \approx 300$ K, the $dd\mu$ molecule is formed by a resonance process in an excited state with the total orbital angular momentum $J = 1$ (see, e.g., [5] for the pioneering papers in theory and experiment). Under these conditions, *dd* fusion proceeds from the $p$-wave of relative deuteron motion, and this fact was intensively exploited in studying nonradiative *dd*-fusion [6–10]. In particular, rates of the $dd\mu$ fusion reactions from a $J = 1$ state, $\lambda_n^f$ and $\lambda_p^f$,

$$dd\mu \to {}^3\mathrm{He} + n + \mu, \quad {}^3\mathrm{He}\mu + n, \tag{2}$$

$$dd\mu \to t + p + \mu \tag{3}$$

were determined experimentally in [9, 10]. The $\mu$CF data allowed extracting the nuclear $p$-wave reaction constants and comparing them with the results of the in-flight data $R$-matrix analysis [11].

Observation of 23.8 MeV $\gamma$-quanta under the conditions of $dd\mu$ resonance formation, i. e., from the $J = 1$ state of the muonic molecule, would unambiguously evidence a $p$-wave contribution to reaction (1). The rate $\lambda_\gamma$ of the radiative capture reaction from the deuteron $p$-wave

$$dd\mu \to {}^4\mathrm{He}\mu + \gamma + 23.8\,\mathrm{MeV}, \tag{4}$$

can be determined by measuring the relative yield of this reaction with respect to main channels (2) and (3),

$$\eta_\gamma = \lambda_\gamma / (\lambda_n^f + \lambda_p^f). \tag{5}$$

The data in [3, 4] allow a rough estimation of the expected yield $\eta_\gamma \approx (5\text{–}10) \cdot 10^{-7}$ [12].

The first experimental search for reaction (1) from the $dd\mu$ molecule was undertaken in our previous measurement [13]. It resulted in the bound $\eta_\gamma < 2 \cdot 10^{-5}$. In this work, we present new measurements with the use of improved methods and experimental techniques.

## 2. REGISTRATION OF THE CAPTURE PROCESS IN THE $dd\mu$ MOLECULE

The $\mu$CF process in deuterium starts when negative muons stop in liquid or gaseous deuterium. At room temperature, the rate of resonant $dd\mu$ molecule formation in the excited state $J = 1$ is [9]

$$\lambda_{dd\mu} = 3.2(3) \cdot 10^6 s^{-1} \phi, \tag{6}$$

where $\phi$ is the deuterium density normalized to the liquid hydrogen density (LHD $= 4.25 \cdot 10^{22}$ nucl/cm$^3$). Fusion reactions (2) and (3) occur with the total fusion rate [10]

$$\lambda_{dd}^f = \lambda_n^f + \lambda_p^f = 407(20) \cdot 10^6 s^{-1}, \tag{7}$$

which is much higher than the free muon decay rate

$$\lambda_0 = 0.455 \cdot 10^6 s^{-1}$$

(the muon lifetime is $\tau_\mu = 1/\lambda_0 \approx 2.2 \mu$s).

After fusion, a muon is released in most cases and can again form a $dd\mu$-molecule, starting a new cycle. The cycles stop either due to a muon decay or to its sticking to fusion products with the effective probability [10]

$$\omega_{dd} = 0.0700 \pm 0.0004. \tag{8}$$

The average number of the $dd\mu$ cycles caused by one muon is estimated as

$$n_c = \frac{\lambda_{dd\mu}\phi}{\lambda_0 + \omega_{dd}\lambda_{dd\mu}\phi}. \tag{9}$$

Fusion events from reaction (4) should arrive after the muon entrance ($t_\mu$) and before the muon decay ($t_e$). The idea of the experimental method consists in a delayed $\mu$–$\gamma$–$e$ coincidence registration. A signal from a delayed electron permits registering the timing gate for signals from the $\gamma$-detectors. This reduces the background significantly. The reaction yield is normalized to the number of muon-decay electrons.

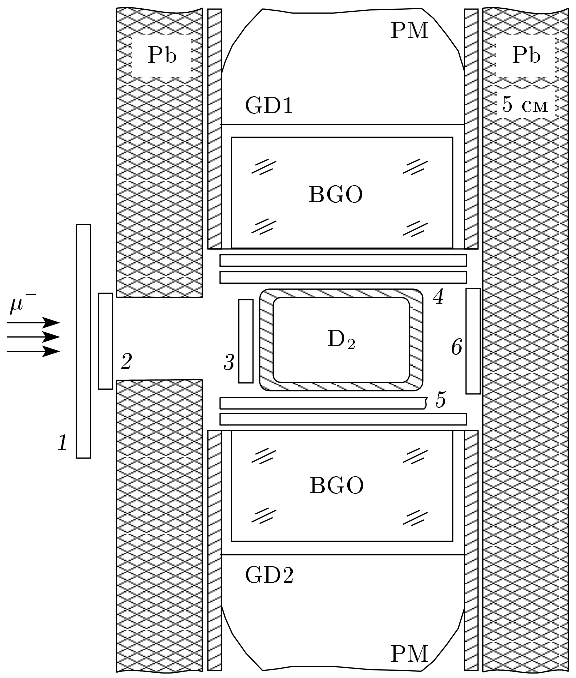


**Fig. 1.** Scheme of the experimental set-up: *1–6*, plastic counters for detection of muons coming to the $D_2$ target and of $\mu$-decay electrons; GD1 and GD2, $\gamma$-detectors; PM, photomultipliers

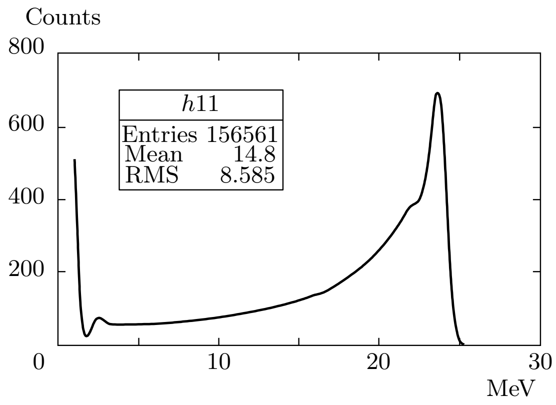


**Fig. 2.** Monte Carlo calculations of the response function of the $\gamma$-detector for $E_\gamma = 23.8$ MeV

## 3. EXPERIMENT

The scheme of the experimental set-up is shown in Fig. 1. The advancement of the set-up compared with [13] was aimed at increasing the $\gamma$-quanta detection efficiency $\epsilon_\gamma$ and at a significant discrimination of the background [14, 15]: we made the set-up as compact as possible and used novel BGO-based $\gamma$-detectors, which combine a high sensitivity $\epsilon_\gamma$ with low efficiency to the background.

A special high-pressure deuterium target with the inner volume 275 cm$^3$ was constructed at VNIIEF [16]. It was filled with deuterium gas from a dedicated source, at the pressure 575 bar corresponding to the deuterium nuclear density $\phi = 0.5$ LHD at the working temperature $T = 290$ K.

### 3.1. Detection and registration system

Two cylinder-shaped electron detectors (*4*, *5*, Fig. 1) (one inside the other) were placed close to the target. This telescope provided a solid angle $\Omega_e \approx 80\,\%$. Some part ($\approx 10\,\%$) of the $\mu$-decay electrons could not pass through the target wall, and hence the total electron registration efficiency was

$$\epsilon_e \approx 0.7 \tag{10}$$

with an accuracy of a few percent.

The main part of the detection system consisted of two large $\gamma$-detectors—BGO crystals 127 mm in diameter and 60 mm in height placed symmetrically around the target (Fig. 1). The total solid angle for both crystals was $\Omega_\gamma \approx 40\,\%$.

The main characteristics of the BGO crystals such as the response, energy calibration, and resolution were studied at VNIIEF [17] with a $^{60}$Co $\gamma$-source (the total energy of two $\gamma s$ $E_{2\gamma} = 2.5$ MeV) and an electrostatic accelerator for producing $\gamma s$ with the energies $E_{\gamma_1} = 16.0$ MeV and $E_{\gamma_0} = 20.4$ MeV in reactions $^{11}\mathrm{B}(p,\gamma_1)^{12}\mathrm{C}^*$ (4.4 MeV) and $^{11}\mathrm{B}(p,\gamma_0)^{12}\mathrm{C}$ at the proton energy 4.9 MeV.

It was established that the linearity of the $\gamma$-detector was kept with an accuracy of (1–2) % within the energy interval 1–20 MeV. The energy resolution function was optimized in accordance with the experimental data. For $\gamma$ energies around 20 MeV, it appeared to be 4 % (FWHM). The absolute efficiency of the $\gamma$-detector was obtained with the known cross section of the reaction $^{11}\mathrm{B}(p,\gamma)^{12}\mathrm{C}$ and the proton flux. The obtained characteristics were remarkably reproduced by GEANT-4. The response function for the $\gamma s$ from process (4) calculated for our real experimental geometry is presented in Fig. 2. The detection efficiency turned out to be

$$\epsilon_\gamma = 15(1)\,\% \tag{11}$$

for the energy interval 20–25 MeV.

To reduce the external background, active shielding (a plastic scintillator shell 7 mm in thickness around each BGO crystal) worked in anticoincidence with the

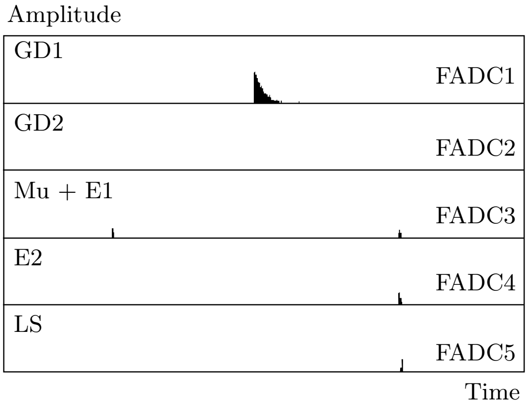


**Fig. 3.** Example of "oscillogramms"—the timing of events in the registration system caused by one muon: FADC1–FADC5 are amplitude channels of the registration system, with the time scale 20 $\mu$s; GD1 and GD2 are signals from the $\gamma$-detectors; Mu+E1 are signals of an incoming muon followed by its decay electron; E2 is the signal of a decay electron; and LS are logic signals to reject accidental background

BGO crystal. Selection of the "pure" BGO signal (without plastic) was realized by comparing the charges for the fast component (30 ns) of the total signal and the slow one (300 ns). This allowed decreasing the background by one order of magnitude without a noticeable loss in the detection efficiency.

The signals from all detectors were directed to flash ADCs (8 bits $\times$ 2048 samples, 100 Mc/s). The trigger checked the presence of the muon stop signal ($\mu$), which was a coincidence $1, 2, 3, (\bar{4} \cdot \bar{6})$, and the electron signal $e$ $(4 \cdot 5)$ in the time interval 4 $\mu$s before $\mu$ and 16 $\mu$s after it. Moreover, the absence of the second incoming muon in the indicated interval was controlled by detector 1. Under these conditions, the data from the flash ADCs were recorded in the PC memory for the further analysis. Some flash ADC signals are shown in Fig. 3.

### 3.2. Measurements

The $D_2$ target was exposed to the negative muon beam (intensity $10^4$ s$^{-1}$, momentum 100 MeV/c) of the JINR Phasotron. The rate of muon stops in the deuterium gas resulting in $\mu$-decay electrons was 200 s$^{-1}$. Additional exposure (with the empty target) was used to determine the electron background.

During the measurements, we used attenuators in the amplitude channels of $\gamma$-detectors. On-line calibration measurements were done with a $^{60}$Co $\gamma$-source without an attenuator. In addition, we checked the calibration observing 5.5 MeV $\gamma s$ from the process $pd\mu \to {}^3\mathrm{He}\mu + \gamma + 5.5$ MeV due to the presence of a 0.5 % protium admixture in the target. The calibration procedure showed a good linearity (not worse than 2–3 %) for the energy response of the $\gamma$-detector.

## 4. ANALYSIS OF THE EXPERIMENTAL DATA

The first step in the analysis of the registered events was the separation of $\mu$-decay electrons $(4 \cdot 5)$ and "pure" $\gamma$-quanta (presence of a signal in the BGO crystal only). Then we accumulated and analyzed the time and charge (energy deposited in the BGOs) distributions of the $\gamma s$. The number of $\mu$-decay electrons necessary for normalizing the $\gamma$ yield was obtained from the analysis of the electron time distribution.

### 4.1. Electron time spectra

Time spectra of electrons from muons that stopped and decayed in the target are distorted by the background originating mainly from muon decays in the target walls. In the run with an empty target, we measured the time spectra of background electrons and obtained the shape of the distribution $B_{empty}(t)$. For the working exposures with a deuterium-filled target, we fitted the electron time spectra taking the background shape into account:

$$N_e^{total}(t) = kB_{empty}(t) + A_e \exp(-\lambda_e t) + F,$$

where $\lambda_e$ is the muon disappearance rate, $F$ is an accidental background, and $k$, $A_e$, $\lambda_e$, and $F$ are fitting parameters. The fitted time distributions of decay electrons for the deuterium-filled and empty target are shown in Fig. 4.

The muon disappearance rate $\lambda_e = 0.465(2)$ $\mu$s$^{-1}$ found from the fit appeared to be close to the free-muon decay rate (7). As a result, the number of electrons from the muon decay in deuterium was obtained:

$$N_e = \frac{A_e}{\lambda_e \cdot \Delta t} \approx 4 \cdot 10^7,$$

where $\Delta t = 20$ ns is the channel bin width. The error of $N_e$ was determined from the uncertainty in fitting the electron time spectra from the filled and empty target and was mainly defined by the total statistics.

### 4.2. Selected $\gamma$-events

We analyzed charge and time distributions of the $\gamma$-events selected with the use of the time criteria [13]

$$0.5\mu\text{s} < t_e - t_\gamma < 2.5\mu\text{s}, \quad 0.5\mu\text{s} < t_\gamma - t_\mu, \tag{12}$$

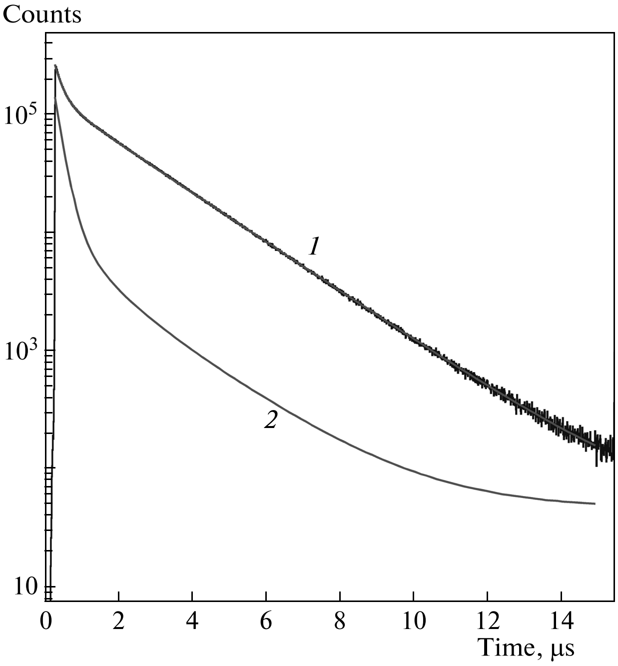


**Fig. 4.** Time spectra of registered electrons for a deuterium-filled target (*1*) and for an empty target (*2*)

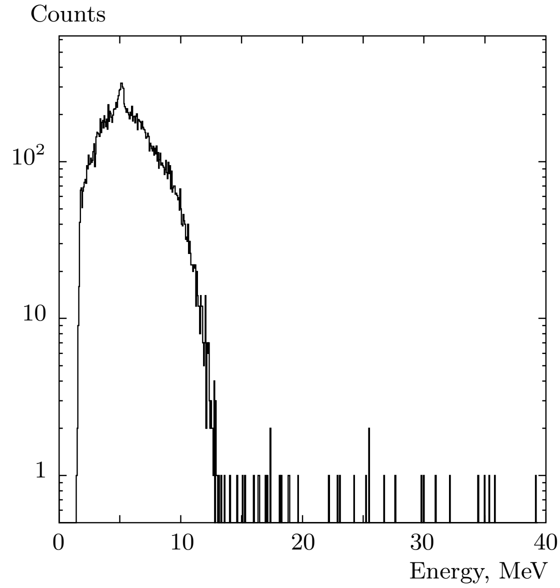


**Fig. 5.** Energy spectrum of the $\gamma s$ accumulated with time criteria (12). The peak at 5.5 MeV from the $pd$ radiative capture reaction is clearly seen

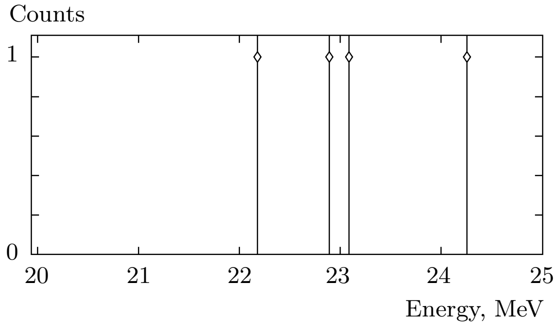


**Fig. 6.** The energy spectrum of the events registered in $\gamma$-detectors, with the selection criteria (12) and (13)

where $t_\mu$, $t_e$, and $t_\gamma$ are the respective times of the muon stop, the electron signal, and the $\gamma$ signal. This selection allowed a radical (by an order of magnitude) suppression of the accidental background. As a consequence, it also decreased the $\gamma$ detection efficiency by the factor $f_t = 0.38$ ($f_t = f_{te} f_{t\mu}$, where $f_{te} = 0.48$ is due to the electron time criterion and $f_{t\mu} = 0.8$ due to the muons). The energy spectrum of events selected by this procedure is shown in Fig. 5.

For the further analysis, we used the energy selection criteria

$$20\,\text{MeV} < E_\gamma < 25\,\text{MeV}. \tag{13}$$

The energy distribution for the selected interval (13) is shown in Fig. 6. We have detected $N_{reg} = 4$ events.

### 4.3. Background estimation

There were two main sources of the $\gamma$-background.

1. An accidental $\gamma$ followed by a real electron (muon decay in deuterium).

2. A bremsstrahlung $\gamma$ (from a $\mu$-decay electron stopped in the target wall) followed by a false $e$-count in the $e$-telescope.

To estimate the background, we analyzed the $\gamma$-signals selected without using criteria (12). This gives an increase of the background events by a known factor (more than one order of magnitude).

The time spectrum of the $\gamma s$ selected in this way and accumulated for energy interval (13) is presented in Fig. 7. The time-independent component is obviously due to the accidental background registered in the $\gamma$-detector. From this component, we derive the mean intensity $n = N/\Delta T$ of the accidental background, where $N$ is the total number of the events in the flat component of the spectrum and $\Delta T$ is the corresponding time interval. Hence, the number $N_{acc}$ of accidental background events satisfying all the selection criteria, including the timing factor $f_t$, is

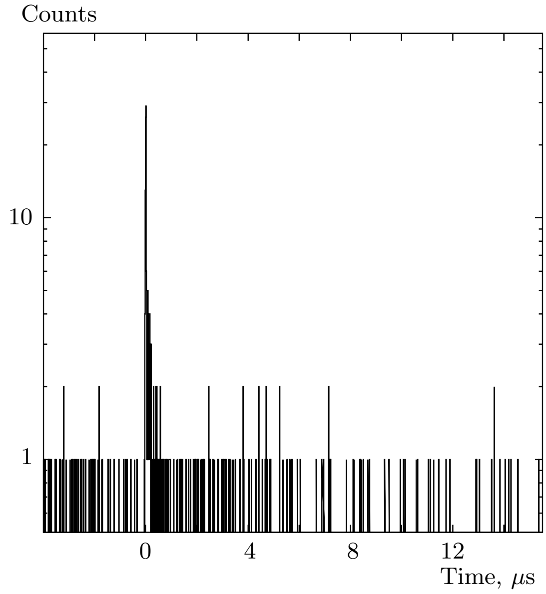


**Fig. 7.** The time distribution of the observed $\gamma$-events for the energy interval 20–25 MeV ("enhanced" background)

$$N_{acc} \approx n\tau_\mu f_t = 2.6. \qquad (14)$$

The correlated background component, i. e., the time-dependent part of the spectrum, is due to the bremsstrahlung followed by a "false" electron. The main source of false electrons is the decay of another muon, stopped in the target before the blocking time interval (earlier than $5\,\mu$s with respect to the muon).

Electron time spectra allow determining the relative probabilities of the accidental electron registration $W_{\gamma\text{-}acc}$ and of the electrons from decay of muons not blocked by a trigger, $W_{\gamma\text{-}e}$. Introducing appropriate enhancement coefficients $K_{\gamma\text{-}acc}$ and $K_{\gamma\text{-}e}$, we can estimate the correlated background $N_{corr}$ for the selection criteria (12) and (13) with the formula

$$N_{corr} = \frac{N_{corr}^{enh}}{W_{\gamma\text{-}acc}K_{\gamma\text{-}acc} + W_{\gamma\text{-}e}K_{\gamma\text{-}e}} \approx 1.4, q \qquad (15)$$

where $N_{corr}^{enh}$ is the number of events in the "enhanced" correlated background. The accuracy in background estimation (15) amounts to 15 %.

## 5. RESULTS

Based on the estimation of the expected background $N_b = N_{acc} + N_{corr} = 4$, we can determine the sensitivity $\alpha$ of our measurements for the 23.8 MeV $\gamma$-detection efficiency $\epsilon_\gamma f_t \approx 0.06$:

$$\alpha = \frac{N_b/\epsilon_\gamma f_t}{N_e n_c} = (6 \div 8)\cdot 10^{-7}, \qquad (16)$$

where $N_e$ is the number of registered electrons and $n_c$ is the average number of $dd\mu$ molecules formed per one muon. Inserting (6), (8), and $\phi = 0.5$ into formula (9), we obtain $n_c$=2.5(1).

With a standard algorithm, we obtain the upper limit for the relative yield $\eta_\gamma$ (5) of reaction (4) with respect to main fusion channels (2) and (3) from the $dd\mu$ state $J = 1$:

$$\eta_\gamma \le 8\cdot 10^{-7} \qquad (17)$$

at the 90 % confidence level.

The upper limit for the radiative fusion rate $\lambda_\gamma^1$ from the $J = 1$ state of the $dd\mu$ molecule can be deduced using the experimental value of the total fusion rate (7) [9, 11]

$$\lambda_\gamma^1 < 3.5\cdot 10^2\,\mathrm{s}^{-1}.$$

## 6. CONCLUSION

In our previous work [13], we estimated the yield of process (4) as a by-product of the main task, the measurement of the $dd\mu$-molecule formation rate [18]. The present experiment is the first serious test in investigating the possibilities of our new technique specially designed for this process. In our run, we have detected $4\cdot 10^7$ $\mu$-decay electrons that correspond to $\sim 10^8$ $dd\mu$-molecule cycles. At the sensitivity level $7\cdot 10^{-7}$, we have detected 4 events satisfying the selection criteria. Following the standard statistical procedure, we deduced the upper bound $8\cdot 10^{-7}$ for the relative yield of reaction (4). This value is close to estimates based on the data in [4].

Further progress may be possible with accumulating larger statistics (by two orders of magnitude). It will allow analyzing the measured energy spectrum as the sum of two background components taken with the known weights and the signal from the studied reaction with the expected shape and variable weight.

The authors gratefully thank M. Yu. Kazarinov, A. P. Kustov, D. Mzhavia, A. G. Olshevsky, Yu. A. Polyakov, N. G. Shakun, and P. T. Shishlyannikov for support in realization of the experiment, and the personnel of the JINR Phasotron and DLNP Electro-Technical Department for works on muon beam delivery. We appreciate useful discussions with C. Petitjean and L. I. Ponomarev.

This work was supported by the RFBR (grants №№ 06-02-16391-a, 08-02-01036-a), and by the INTAS (grant № 7953).

## REFERENCES

1. F. J. Wilkinson and F. E. Cecil, Phys. Rev. C **31**, 2036 (1985).
2. C. A. Barnes, K. H. Chang, T. R. Donoghue et al., Phys. Lett. B **197**, 315 (1987).
3. L. H. Kramer, R. M. Chasteler, E. Hayward et al., Phys. Lett. B **304**, 208 (1993).
4. K. Sabourov, M. W. Ahmed, S. R. Canon et al., Phys. Rev. C **70**, 064601 (2004).
5. E. A. Vesman, Pis'ma v Zh. Eksp. Teor. Fiz. **5**, 113 (1967); S. I. Vinitsky et al., Zh. Eksp. Teor. Fiz. **79**, 698 (1980); V. M. Bystritski et al., Pis'ma v Zh. Eksp. Teor. Fiz. **31**, 249 (1979); Phys. Lett. B **94**, 476 (1980); Zh. Eksp. Teor. Fiz. **80**, 1700 (1981).
6. L. N. Bogdanova, V. E. Markushin, V. S. Melezhik et al., Phys. Lett. B **115**, 171 (1982), Erratum B **167**, 485 (1986).
7. D. V. Balin, E. M. Maev, V. I. Medvedev et al., Phys. Lett. B **141**, 173 (1984); Pis'ma v Zh. Eksp. Teor. Fiz. **40**, 318 (1984).
8. D. V. Balin, A. I. Ilyin, E. M. Maev et al., Muon Cat. Fusion **1**, 127 (1987).
9. C. Petitjean, D. V. Balin, W. H. Breunlich et al., Hyp. Int. **118**, 127 (1999).
10. N. I. Voropaev, D. V. Balin, W. H. Breunlich et al., Hyp. Int. **138**, 331 (2001).
11. G. M. Hale, Muon Cat. Fusion **5**/**6**, 227 (1990/1991).
12. L. N. Bogdanova and V. V. Filchenkov, Hyp. Int. **138**, 321 (2001).
13. L. N. Bogdanova, V. R. Bom, D. L. Demin et al., Yad. Fiz. **65**, 1826 (2002).
14. L. N. Bogdanova, Yu. I. Vinogradov, N. N. Grafov et al., in *Book of Abstr. 56$^{th}$ Int. Conf.* "*Nucleus-2006*", Sarov (2006), p. 253.
15. D. L. Demin, V. V. Filchenkov, N. N. Grafov et al., in *Proc. Int. Conf. on Muon Catalyzed Fusion and Related Topics*, "$\mu$CF-07", Dubna, JINR (2008), p. 294.
16. V. V. Perevozchikov, A. A. Yukhimchuk, Yu. I. Vinogradov et al., Hyp. Int. **138**, 417 (2001).
17. L. N. Generalov, B. L. Lebedev, K. L. Mikhailyukov et al., Preprint VNIIEF, 104-2009, Sarov, Russia (2009).
18. V. R. Bom, D. L. Demin, C. W. E. van Eijk et al., Zh. Eksp. Teor. Fiz. **123**, 518 (2003).